Image Acquisition and Process Variable Measurement System for Weld Deposition Evaluation

Bryan Stefan Galani Pernambuco, Cristiano Rafael Steffens and Silvia Silva da Costa Botelho
Federal University of Rio Grande
Computational Sciences Center
Rio Grande - RS, Brazil
http://c3.furg.br

***Abstract*—Understand and improve weld deposition is a key challenge to upgrade the overall metallic welding process. However controlling and understanding the welding process is still an open challenge. In order to study the phenomenon involved in the metallic transfer we employ a high-speed camera and laser lighting equipment to record the deposition images using the shadowgraph technique. Combining the image acquisition setup with voltage, current and wire speed data, we were able to obtain a dataset of different welding conditions, which allow us to observe critical aspects of the deposition. We present a software based on computer vision that makes possible to analyze each frame from a recorded welding, providing per sample statistics, frame's stats and a framework to save and show annotations of the due video. Through visual information and inferential statistics we were able to identify the transfer mode used and how the parameters influence the weld of steel plates. Furthermore, we believe the tools provided, will enable researchers to evaluate the process and foster the development of hardware, software and control techniques related to the field.**

Keywords*—*Weld, Computer Vision, Upgrading Welding Process, Measurements, Statistical Functions.

I. INTRODUCTION

Metallic welding performs an important role in manufacturing and construction industries. Understanding and properly controlling the metallic deposition are goals that have been studied for a long time [1]. Research in fields such as material science, metallurgical engineering, production engineering, and manufacturing technology have contributed to the development of technologies and techniques that enabled the welding industry to improve its effectiveness and drastically reduce the material waste.

According to [2], there are three major types of fusion welding process: *i.* Gas Welding, *ii.* Arc Welding, *iii.* High-Energy Beam Welding. Pohanish *et al.* [3] claims there are among one hundred welding and allied processes. In this paper, we are interested in the arc welding process, which uses the fusion of the base metal to make the weld. The electric arc presents a good combination of characteristics, such as the small cost of equipment, the small health risk to operators and its ease control [4].

For the tests made in this paper we used the Gas Metal Arc Welding (GMAW) process, which is one of the most popular welding processes, once its simple setup makes it suitable for both shop-floor and field welding. Sometimes referred to by the gases that protect the arc and weld pool, MIG (Metal Inert Gas) or MAG (Metal Active Gas). GMAW is an arc welding process in which an electric arc forms between a continuous metal electrode (consumable wire) and the work-piece [5], which heats the work-piece and the consumable wire causing them to melt and join.

The MIG/MAG welding process is normally executed using Reverse Polarity (CC+). In Reverse Polarity the plate is negatively charged and the electrode positively charged [6]. According to [7], the use of Direct Polarity (CC-) is limited to globular transfer mode and is barely used because it produces undesired spatter, the resulting arc is unstable, and the droplet becomes asymmetric due to a repulsive cathodic force that acts on the fused end of the electrode in response to the electron flow [8].

The welding arc is an electric current conductor, therefore, the electric current interacts with the electromagnetic field produced by itself. This interaction generates some effects that could enhance or damage the weld [9]. In some cases, depending on how the current enters in the weld puddle the electromagnetically induced flow can turn toroidal, leading the weld pool to rotate [10]. This effect occurs only when the weld pool is almost hemispherical, that means, its format looks like half of a sphere. This geometry occurs when welding using TIG (Tungsten Inert Gas) at low current [10].

Gas Metal Arc Welding can be classified in three main transfer modes:

- Short-Circuit, in which the consumable wire is melted in the weld puddle through fast and successive contacts, in each short-circuit the current values tend to increase and the voltage values tend to decrease, extinguishing the electric arc and transferring the drop to the weld puddle [11].
- Spray, is characterized by a continuous flow of fine droplets and vaporized metal from the electrode to the work-piece rapidly, as the current increases, the diameter of the droplet decreases causing an increase in the transfer frequency [4].
- Globular, is a transfer mode between the short-circuit

and the spray in which large drops of liquid wire are released at low frequency from the electrode end, mainly due to the gravitational force [4]. The radius of the drop can be up to 1.5 times greater than the radius of the wire.

The welding process has several variables to indicate critical information about controlling it, as the dynamical change in weld pool surface [12] and the quality of the equipment that was used [13]. A properly adjusted level of current, voltage and wire speed avoids smoke, welding spatter, and deformation. For instance, the spray mode should not be used to weld thin plates due to their high current requirement, while short-circuit transfer is generally used to weld thin plates due to their low current and voltage level. Finally, the globular transfer mode is the most undesirable because it has many spatter, high heating and lower welding quality [14]. Therefore, each transfer mode has its limitations and should be carefully chosen by the operator in order to produce acceptable results.

We propose an acquisition system and a computer vision based software that allows a frame-by-frame analysis of a recorded welding, combined with a multi-scalar graphic that shows the behavior of the values of current, voltage and wire speed and how the change of this values interfere in the video. To improve the understanding of the variables, a board with statistical techniques was inserted, for instance, median, mode, standard deviation, skewness, and kurtosis. With our results, the operator can achieve the best-configured parameters for improving and mastering the welding process.

Datasets play a fundamental role in the development and validation of new models and techniques. Datasets such as [15], [16] and [17] laid the foundation to improve the development of their respective areas. More recent works such as [18], [19], brought significant enhancement, combining reliability and knowledge to new and larger databases.

II. ACQUISITION SYSTEM

The acquisition system is composed of two main arrangements: Image Acquisition and Data Acquisition. For the data acquisition, we used a micro-controller to store and process data about the electrical variables of the process, a current transducer, a voltage transducer, and an incremental encoder, as can be observed in Figure1. Aiming to assist in the understanding of the deposition process and overcome the challenges posed by the light produced by the welding process, to obtain the images used in the remaining part of this paper, we made use of a Phantom Miro 311 high-speed camera, manufactured by Vision Research Inc., a Cavilux high-power laser illumination system manufactured by Cavitar Ltd., and a narrow band optical filter. The image acquisition equipment was positioned in two arrangements as shown in Figures 2 and 3.

A. Shadowgraph Imaging

One of the arrangements used for image acquisition was the shadowgraph method [20], also known as back-lighting, which makes it possible to observe the contours of the welding joint, consumable wire and weld puddle. This technique basically consists of the positioning of a high-speed camera synchronized with a laser and a micro-controllable circuit as can be observed in Figure 4.

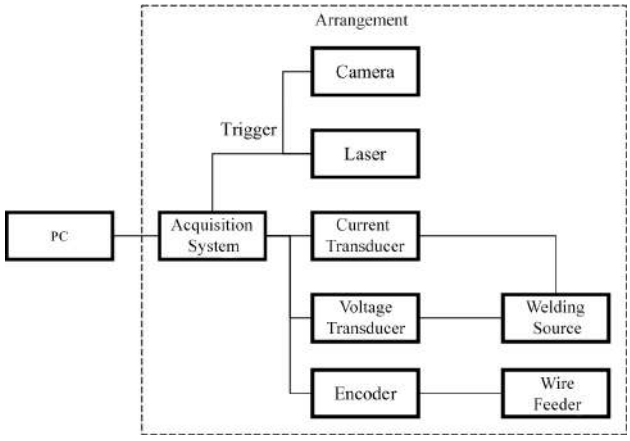

Fig. 1. Abstraction of the arrangement used for image acquisition in synchrony with the electrical quantities of the process.

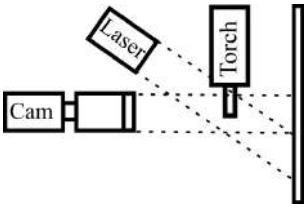

Fig. 2. The technique of imaging using frontal illumination allows visualizing information of brightness and detachment of gases. Allows welding visualization within the butt welding joints.

Due to the high brightness coming from the electric arc, the laser must be positioned so that it exceeds the brightness of the weld. The beam of light emitted by the laser is enlarged with the aid of divergent and convergent lenses, which illuminates only the region of interest and generates as input to the camera the shadow of the process.

In this experiment a wavelength of 640 $\pm$ 10 nm was used at a frequency of 1 kHz or 3 kHz with an energy pulse of 500 Watts. Combined with a band-pass optical filter. The camera has also been set to a frequency of 1 kHz or 3 kHz. The images acquired with shadowgraph method facilitate the digital image processing, since they are gray-scale and present high contrast between the background and the foreground, usually filled in black (wire, molten wire, droplet, and pool shadow) or white (laser light that passes through the filter and reaches the sensor of the camera) as it can be observed in Figure 3.

B. Frontal Imaging

The other arrangement used was the frontal imaging, which consists in the utilization of both the camera and the laser in

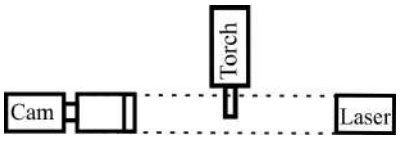

Fig. 3. The technique of imaging using shadowgraph allows the visualization of the wire's contour, droplet, and weld puddle. Its application is restricted to welding on sheet metal..

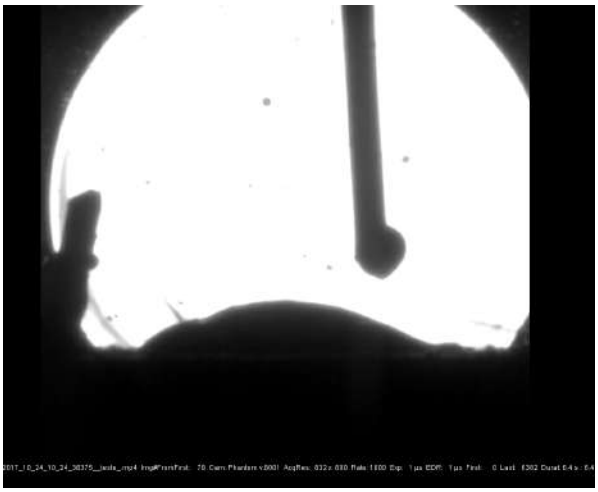

Fig. 4. Image obtained by shadowgraph method.

the front part of the welding process as observed in Figure 2, allowing a real view of the weld transfer and not of its shadow. This technique is most used to observe the phenomena generated in the process such as the shielding gas, the droplet asymmetry, the electron flow and the pool surface as can be seen in Figure 5.

Fig. 5. Image obtained by frontal illumination

C. Microcontrolled Circuit

The micro-controlled circuit is composed of one micro-controller to store and process the obtained data, two transducers, where one of them is used to obtain the current values and the other one voltage values [21]. And an incremental encoder to collect the wire speed, converting the position of one rotation to a digital output through opening and closing the contacts [22]. A signal conditioning circuit is applied to adjust the inputs to logic levels supported by the micro-controller, as well as to synchronize the data collected from the transducers with a global clock signal provided by the camera.

III. DATA ANALYSIS SYSTEM

For the construction of the Data Analysis system, we used the IDE (Integrated Development Environment), QT Creator, which is a multi-platform working environment used to develop interfaces using the C ++ programming language created by Norwegian company Trolltech. The language used, C ++ [23], was initially developed by Bjarne Stroustrup and has become one of the most popular commercial languages since the 1990s because of its great performance and user base. Several libraries were used in this software, highlighting OpenCV and GNU C Library - GLIBC.

The OpenCV Library is mainly used for the area of computer vision, having image and video processing modules, data structure, Linear algebra, basic GUI with independent windows system, mouse and keyboard control, and more than 350 computer vision algorithms such as image filters, camera calibration, object recognition, structural analysis and others [24], [25].

Another library used was the GNU C Library- GLIBC distributed under the GNU Lesser General Public License, which provides implementations of statistical functions. Basic statistical functions include routines for averaging, variance, and standard deviation. More advanced functions allow you to calculate absolute deviations, slope, and kurtosis, as well as the median and arbitrary percentiles. Algorithms use recurrence relations to calculate mean quantities in a stable manner, without large intermediate values that can cause excessive flow [26].

A. Statistics

1) Arithmetic Average: The mean, or arithmetic average, is an estimate of the value at which the values in a sample tend to concentrate. The mean is given by Eq. 1, where *n* is the number of samples points and X_i is the sample. In general, the mean provides a good estimate of the central point [27]. However, depending on the data distribution and outliers, it might provide unrealistic values.

$$\overline{X} = \sum_{i=1}^{n} \frac{X_i}{n} \tag{1}$$

2) Median: The median is a measure of central tendency and separatrix. Its function is to divide the series, already ordered, into two equal parts, each part containing the same quantity of elements [28]. The median is given by Eq. 2, where P_{Md} is the position of the median and *n* is the number of sample.

$$P_{Md} = \frac{n+1}{2} \tag{2}$$

The median provides a more accurate measure of central tendency in sets of data which are rigged due to outliers. Under a normal distribution, mean and median should lie close to each other. However, under conditions where a few sample points are not evenly distributed, the mean may provide a better measure to describe the welding process.

3) Standard Deviation: The standard deviation provides a good idea of the variation among the sample points. It is useful to classify the process among several metal transfer modes, as well as to determine the overall quality and stability of the process. As with the mean, the standard deviation is a weak measure because it is influenced by values either very large or very small. The higher the standard deviation, the greater the variation (dispersion) between the values [29]. More homogeneous sets have smaller standard deviations.

$$s = \sqrt{\frac{1}{n-1}\sum_{i=1}^{n}(X_i - \overline{X})^2} \tag{3}$$

The standard deviation is given by Eq. 3, where $\overline{X}$ is the Arithmetic Average, *n* is the number of sample points and X_i is the value of each sample.

4) Pearson's Correlation Coefficient: Pearson's correlation coefficient is a measure of the linear correlation between two random variables X and Y. It has a range of values between $+1$ and -1, where 1 stands for total positive correlation, 0 stands for no linear correlation between the two variables, and -1 stands for total negative linear correlation [30]. Pearson's Correlation Coefficient is defined by Eq. 4, where $cov(X, Y)$ is the covariance of the element X and the element Y. s_x and s_y are the standard deviations of the element X and the element Y.

$$P_{x,y} = \frac{cov(X, Y)}{s_x s_y} \tag{4}$$

In our application, the correlation provides insights about the dependencies within the welding variables and the observed behavior. We recall that the electric arc welding deposition process follow Ohm's Law, where voltage, current, and resistance are intrinsically related. However, as the power source is not ideal, the resistance is a direct result of the electrical arc length, many effects, such as capacitance, magnetic fields, and effects of the conductive fluids (plasma), cannot be modeled following only Ohm's assumptions.

5) Skewness Coefficient: When a distribution ceases to be symmetrical, the mode, median, and mean move away from the central point, increasing the difference between them [28]. The skewness measures the asymmetry of the tails of a distribution as given by the Eq. 5.

$$As = \frac{1}{n}\sum\left(\frac{X_i - \overline{X}}{s}\right)^3 \tag{5}$$

A null value indicates that the values are distributed fairly evenly on both sides of the mean. The classification of the asymmetry can be seen below.

- Positive Skew, a negative value indicates that the tail on the left side of the probability density function is larger than the right side.
- Negative Skew, a positive value for asymmetry indicates that the tail on the right side is larger than on the left side.

6) Kurtosis: Kurtosis indicates how much the frequency curve of a distribution is sharper or flatter than a standard (symmetric) normal curve [31]. The kurtosis is calculated by 6 where Q_3 and Q_1 are the quartiles and P_{90} and P_{10} are the percentiles.

$$K = \frac{(Q_3 - Q_1)}{2(P_{90} - P_{10})} \tag{6}$$

The quartiles (Q) are the division of the ordered series in four equal parts, each one will have 25% of its values. The percentiles (P) are the division of the ordered series in 100 equal parts, in which each part gets 1% of its values. So 1% is on your left and 99% on the right [28].

According to the value of kurtosis, we can have three types of frequency curves:

- Mesokurtic, $K = 0,263$, when the frequency curve has a flattening tail equivalent to that of the standard curve.
- Leptokurtic, $K < 0,263$, when the frequency curve has thicker tail, higher than the standard curve.
- Platykurtic, $K > 0,263$, when the frequency curve shows a higher flattening tail, higher than the standard curve.

These types of frequency curves can be observed in Figure 6.

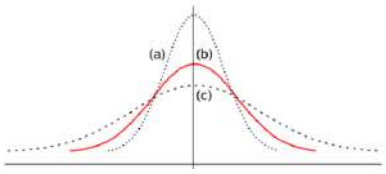

Fig. 6. Frequency Curves, according to the value of kurtosis. Where the curve (a) is Leptokurtic, (b) is Mesokurtic and (c) is Platykurtic.

The visualization tool for acquired images contains some general restrictions such as:

- Files may have an arbitrary number of sample points. There are no rigid sample size limits involved.
- The smallest number of samples restricts the data that is shown.
- Video playback stops when the user clicks the add comment button, to keep watching the user should click the play button.
- If a comment is added in the same frame in which another already exists, it will be overwritten.
- If a data file is not provided by the user, the program will show a warning message.

In addition, the visualization tool has control of the playback speed of the video (frames per second), a check box that allows the synchronization of the graphic values with the video, a start button and a stop button, a forward button to advance 10 frames and another to go back 10 frames, a button

to add a comment in the frame (that will be saved in the same directory of the video in a CSV file (Comma-separated values), making it easier to handle) and a last button to remove all comments from the video (remove all annotations from the CSV file).

The software also displays statistical calculations provided by the video and the tests, including the limit data of the files, mean and standard deviation of current and voltage, average wire speed, the correlation between electric current and voltage, current and wire speed, the auto-correlation of voltage and current. In addition to these variables, the proposed software computes data from the current frame, such as average brightness, median, standard deviation, slope, kurtosis and a gray-scale image histogram. All wire current, voltage, and velocity values are plotted on a multi-scale chart that may or may not be reproduced in sync with the video.

The flowchart shown in Figure 7, depicts the order of execution of the visualization tool modules that can be divided into 4 major steps:

- The first one to be executed is the one of processing, that carries the files with the values of current, tension and speed of the wire, verifying their existence and associating the video with the comments.
- The second computes the static values based on the inserted data and renders the graphs.
- The third module is responsible for processing the video itself, loading the video, extracting the characteristics of the image and computing the data of the frame.
- The fourth and last module is responsible for the display, where the rendering of images and annotations occurs and displays them on the interface.

IV. RESULTS

For the validation of the functionality and reliability of the software, more than 20 weld videos were evaluated, being 7 of frontal illumination and 14 using shadowgraph, alternating between the modes of globular transfer, short circuit, and spray. In the Figures 8 and 9 we can observe the statistical data from the whole test and individual frame displayed at the developed visualization tool and a graph of the values of voltage (red), current (blue) and wire speed (green), respectively.

The processing time for the four software modules takes about 42 seconds on a conventional computer. The Figures 10 and 11 were collected from a GMAW welding process with Reverse Polarity (CC+), in which the plate is negatively charged and the electrode positively charged. The inverse polarity acts so that the electron flow is generated in the inverse direction of the gravitational force, incurring a higher melt rate and a concentration of arc heat in the base [8]. The welding machine acts to control the voltage level. The current variation occurs primarily as a function of the electric resistance in the arc.

Through the analysis of the data obtained by the tool, it becomes possible to observe the voltage and current peaks and to make corrections in the next welding process. In addition,

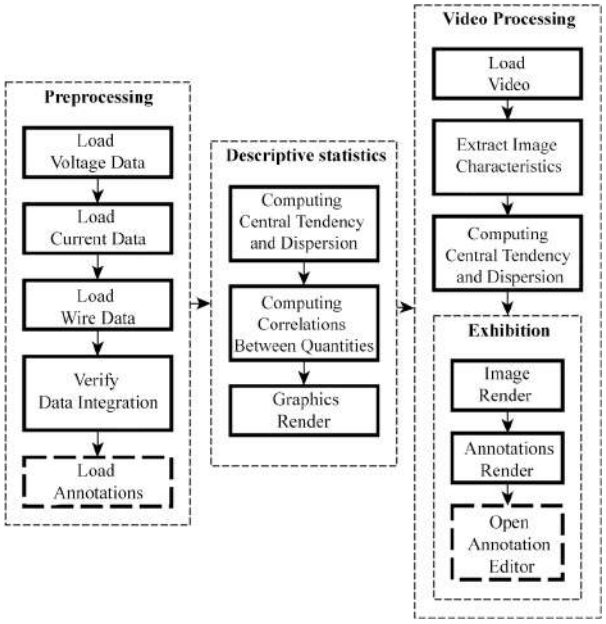

Fig. 7. The developed Data Analysis System allows to load, validate and compute descriptive statistics measures. The rendering of the video and the graphs of the electric quantities allows the researcher to identify the occurrence of phenomena of interest.

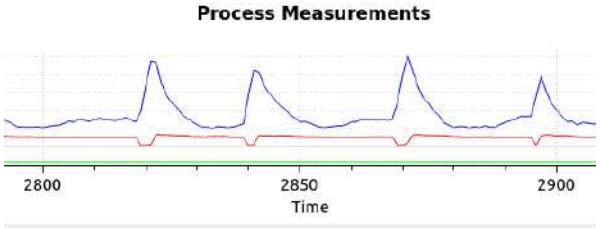

Fig. 8. Graph of voltage values in volts (red), current in amperes (blue) and wire speed in meters per minute (green).

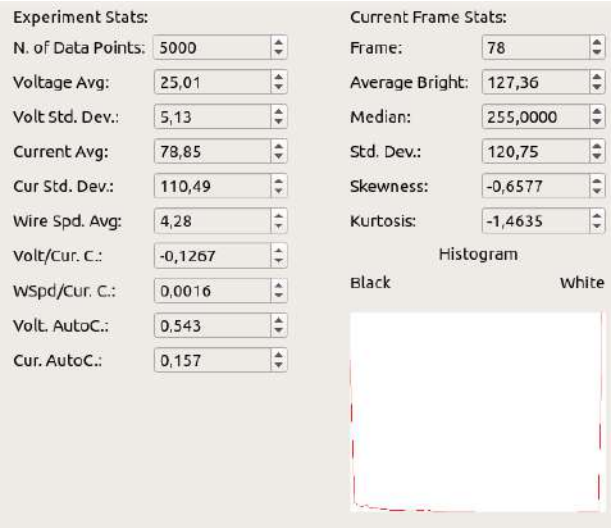

Fig. 9. The display of frame statistics in the visualization tool. It can be seen that the average voltage during the welding was 25 volts, which is regulated in a stable manner by the welding source. The current has a standard deviation greater than the average in function of the short-time peaks in the short-circuit when it closes contact between the electrode and the work-piece.

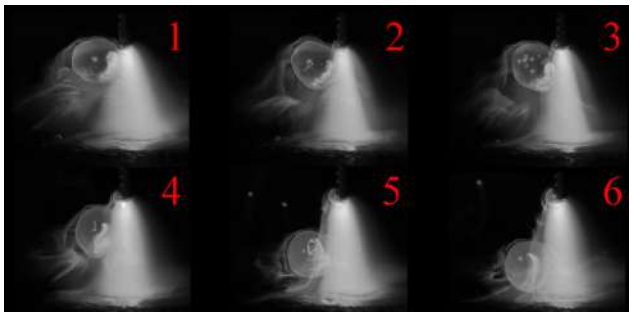

Fig. 10. A sequence of frames showing the formation and detachment of the drop using globular transfer mode in GMAW welding process with inverted polarity. Sequence allows visualization of the forces acting on the detachment.

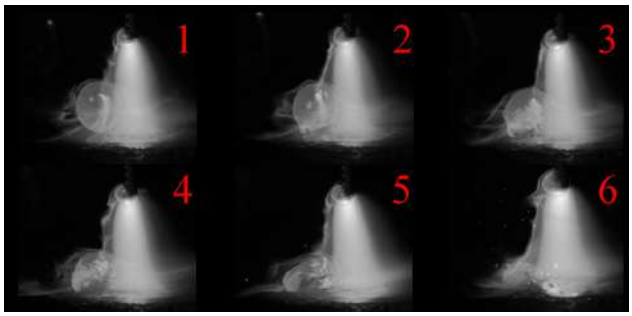

Fig. 11. A Sequence of frames showing the contact of the droplet with the work-piece (puddle of molten material) in GMAW welding process.

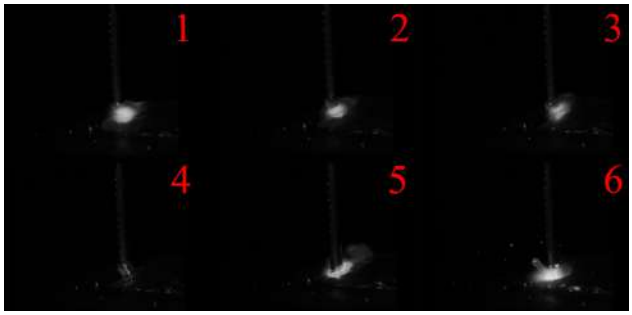

Fig. 12. A sequence of frames showing the formation and detachment of the drop using short-circuit transfer mode in GMAW welding process with inverted polarity. Sequence allows visualization of the forces acting on the detachment.

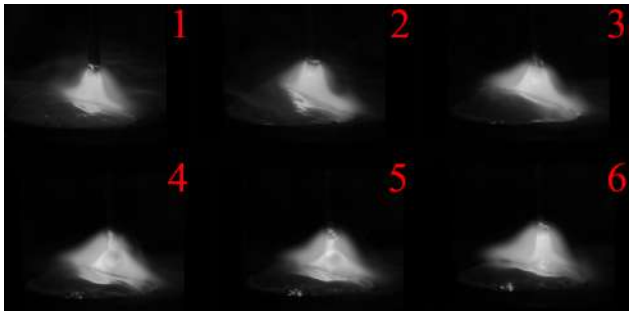

Fig. 13. A sequence of frames showing the formation and detachment of the drop using spray transfer mode in GMAW welding process with inverted polarity. Sequence allows visualization of the forces acting on the detachment.

it enabled the observation of the wire's droplet detachment phenomena and the contact of the same with the plate such as the electron flow, the repulsive force acting upward in the drop due to the emission of electrons, which justifies the droplet being asymmetrically repelled [8]. Such phenomena can be clearly seen in the Figures 10 and 11, which were welded using globular transfer mode.

The different configurations of the levels of current, voltage and wire speed affect directly the behavior of the phenomena as could be seen comparing the Figures 10, 12 and 13. Some visual differences that could be observed are the size of the electron flow, the different drop asymmetry for each mode, and the accumulation of molten wire at the tip of the electrode. The images were acquired using three different transfer mode, globular, short-circuit and spray.

The results presented in the data analysis system also collaborate in the validation of models such as [32], as shown in the Figures 8, 9 , 2 and 4. Our dataset includes both direct polarization and inverse polarization. Data was collected using three main weld deposition modes including spray, short-circuit, and globular transference. On one side, we notice that images obtained through the shadowgraph method present sharp and well-defined edges that provide a clear visualization of the melted wire and the welding pool. Images obtained using frontal illumination, on the other side, provide additional data on the behavior of the gases, fumes and ion flow.

V. CONCLUSION

Through the literature review of transfer modes and electric quantities of the welding process, it was possible to identify the potential of studying the variables used in the GMAW weld deposition process. In this sense, the contribution of our research is related to the analysis and visualization of the parameters that were generated by the process, through image acquisition, computer vision techniques and a system for synchronized variable measuring. Through the use of the acquisition system and the software artifact presented, welding researchers can evaluate the process and promote the development of hardware, software, control techniques, and robotic systems related to the field.

In future work, we intend to implement segmentation, detection and classification algorithms through the droplet image, in order to upgrade the visualization tool with substantial information about the weld deposition, such as the droplet's centroid, diameter and detachment speed. The extraction of that information allows a wide study about the welding process, encompassing evaluation of the drop movement in transfer [33] and evaluation of the influence of the current pulse, time of pulsing, transference, as well as the robot's end-effector position and movement.

REFERENCES

[1] A. I. H. Committee and D. Olson, *ASM handbook: Welding, brazing, and soldering*, ser. ASM Handbook. ASM International, 1993. [Online]. Available: https://books.google.com.br/books?id=y0VLAQAAIAAJ

[2] S. Kou, *Welding metallurgy*. John Wiley & Sons, 2003.

[3] R. Pohanish, *Glossary of Metalworking Terms*. Industrial Press, 2003. [Online]. Available: https://books.google.com.br/books?id=6zTREw5lrjMC

[4] P. J. Modenesi, "Introdução à física do arco elétrico e sua aplicação na soldagem dos metais," *Belo Horizonte*, 2007.

[5] P. J. Modenesi, P. V. Marques, and D. B. Santos, "Introdução à metalurgia da soldagem," *Belo Horizonte: UFMG*, 2012.

[6] C. FORTES and C. Vaz, "Apostila eletrodos revestidos," *Elektriska Svetsnings Aktie Bolaget (ESAB)*, 2005.

[7] J. E. Talkington, "Variable polarity gas metal arc welding," Ph.D. dissertation, The Ohio State University, 1998.

[8] D. Souza, A. Resende, and A. Scotti, "Um modelo qualitativo para explicar a influência da polaridade na taxa de fusão no processo mig/mag," *Soldagem e Inspeção (Impresso)*, vol. 14, pp. 192–198, 2009.

[9] M. M. NERIS, "Soldagem dos metais," http://cursos.unisanta.br/mecanica/solda.html, 2002.

[10] J. F. Lancaster, "The physics of welding," *Physics in technology*, vol. 15, no. 2, p. 73, 1984.

[11] D. Souza, M. L. Rossi, F. Keocheguerians, V. NASCIMENTO, V. VILARINHO, and A. Scotti, "Influência da tensão de soldagem e do gás de proteção sobre a correlação entre indutância e regularidade da transferência metálica na soldagem mig/mag por curto-circuito," *Soldagem e Inspeção, São Paulo*, vol. 16, no. 2, pp. 114–122, 2011.

[12] G. Saeed and Y. Zhang, "Mathematical formulation and simulation of specular reflection based measurement system for gas tungsten arc weld pool surface," *Measurement Science and Technology*, vol. 14, no. 9, p. 1671, 2003.

[13] C. R. Steffens, V. Huttner, B. L. Quaresma, V. S. Da Rosa, and S. S. D. C. Botelho, "Fpga based sensor integration and communication protocols for automated robot control in linear welding," in *Robotics Symposium and IV Brazilian Robotics Symposium (LARS/SBR), 2016 XIII Latin American*. IEEE, 2016, pp. 115–120.

[14] E. G. Ramos, "Análise da oscilação da poça de solda em gmaw por meio de processamento de imagens obtidas por perfilografia," Ph.D. dissertation, Universidade de Brasilia, 2012.

[15] A. Krizhevsky, I. Sutskever, and G. E. Hinton, "Imagenet classification with deep convolutional neural networks," in *Advances in neural information processing systems*, 2012, pp. 1097–1105.

[16] G. A. Miller, "Wordnet: a lexical database for english," *Communications of the ACM*, vol. 38, no. 11, pp. 39–41, 1995.

[17] Y. LeCun, "The mnist database of handwritten digits," *http://yann. lecun. com/exdb/mnist/*, 1998.

[18] U. Consortium, "Uniprot: the universal protein knowledgebase," *Nucleic acids research*, vol. 45, no. D1, pp. D158–D169, 2016.

[19] T.-Y. Lin, M. Maire, S. Belongie, J. Hays, P. Perona, D. Ramanan, P. Dollár, and C. L. Zitnick, "Microsoft coco: Common objects in context," in *European conference on computer vision*. Springer, 2014, pp. 740–755.

[20] C. C. Rusu, L. R. Mistodie, and E. Ghita, "Laser shadowgraph system for the electrical arc investigation," *University" Politehnica" of Bucharest Scientific Bulletin, Series D: Mechanical Engineering*, vol. 73, no. 2, pp. 189–198, 2011.

[21] V. Hüttner, D. D. de Paula, L. C. M. Pereira, E. do Amaral Leivas, C. R. Steffens, and S. S. da Costa Botelho, "Welding turns digital: Electronics and fpga-based design to actuate a linear welding work cell," *Revista Jr de Iniciação Científica em Ciências Exatas e Engenharia*, vol. 14, 2016.

[22] C. Platt, *Encyclopedia of Electronic Components Volume 1: Resistors, Capacitors, Inductors, Switches, Encoders, Relays, Transistors*. " O'Reilly Media, Inc.", 2012, vol. 1.

[23] M. A. Ellis and B. Stroustrup, *The annotated C++ reference manual*. Addison-Wesley, 1990.

[24] I. Itseez, "Open source computer vision library," https://github.com/itseez/opencv, 2015.

[25] ——, "The opencv reference manual," https://docs.opencv.org/3.0-beta/opencv2refman.pdf, April 2014.

[26] B. Gough, *GNU scientific library reference manual*. Network Theory Ltd., 2009.

[27] W. O. Bussab and P. A. Morettin, *Estatística básica*. Atual São Paulo, 1986.

[28] P. A. Barbetta, M. M. Reis, and A. C. Bornia, *Estatística: para cursos de engenharia e informática*. Atlas São Paulo, 2004, vol. 3.

[29] S. S. PINTO and C. S. d. SILVA, "Estatística vol. i," 2013.

[30] J. Benesty, J. Chen, Y. Huang, and I. Cohen, "Pearson correlation coefficient," in *Noise reduction in speech processing*. Springer, 2009, pp. 1–4.

[31] P. A. Morettin and W. O. Bussab, *Estatística Básica* . Editora Saraiva, 2000.

[32] P. J. D. de Oliveira Evald, J. L. Mór, C. R. Steffens, S. S. da Costa Botelho, and R. Z. Azzolin, "Modelagem das dinâmicas da formação da gota e transferência de massa em processos de soldagem à arco," in *Congresso Brasileiro de Automática*, vol. 1, no. XXI. Sociedade Brasileira de Automática, 2016, p. 6.

[33] C. E. A. L. Rodrigues and A. Scotti, "Levantamento e avaliação do movimento de gotas em transferência na soldagem mig/mag," *POSMEC/UFU - Simpósio do Programa de Pós-Graduação em Engenharia Mecânica*, 2004.